

Fabrication of lateral single-electron tunneling structures by field-induced manipulation of Ag nanoclusters on a silicon surface

Kang-Ho Park, Mincheol Shin, Jeong Sook Ha, Wan Soo Yun, and Young-Jo Ko

Citation: *Appl. Phys. Lett.* **75**, 139 (1999); doi: 10.1063/1.124326

View online: <http://dx.doi.org/10.1063/1.124326>

View Table of Contents: <http://apl.aip.org/resource/1/APPLAB/v75/i1>

Published by the [American Institute of Physics](#).

Additional information on *Appl. Phys. Lett.*

Journal Homepage: <http://apl.aip.org/>

Journal Information: http://apl.aip.org/about/about_the_journal

Top downloads: http://apl.aip.org/features/most_downloaded

Information for Authors: <http://apl.aip.org/authors>

ADVERTISEMENT



Goodfellow
metals • ceramics • polymers • composites
70,000 products
450 different materials
small quantities fast

www.goodfellowusa.com

Fabrication of lateral single-electron tunneling structures by field-induced manipulation of Ag nanoclusters on a silicon surface

Kang-Ho Park,^{a)} Mincheol Shin, Jeong Sook Ha, Wan Soo Yun, and Young-Jo Ko
Telecommunications Basic Research Laboratories, ETRI, Yusong P.O. Box 106, Taejeon 305-600,
Republic of Korea

(Received 12 January 1999; accepted for publication 13 May 1999)

Nanostructures composed of Ag clusters on an Sb-terminated Si surface were designed in a highly controlled manner and the electric conduction through Ag nanoclusters to the silicon substrate was investigated by using a scanning tunneling microscopy/spectroscopy. It was found that the lateral conduction between neighboring Ag clusters significantly contributed to the tunneling current–voltage characteristics, and the metallic single-electron tunneling structures employing the lateral conduction channels at room temperature can be fabricated via a field-induced manipulation of Ag clusters. © 1999 American Institute of Physics. [S0003-6951(99)04627-6]

The metal nanoclusters formed on semiconductor surfaces have been intensively investigated in terms of the nanoscale Schottky barrier formation^{1–3} and the onset of metallicity with a variation of cluster size.^{4,5} Very recently, there have been several reports on the measurements of single-electron phenomena in metal nanoclusters formed on silicon surfaces by using a scanning tunneling microscopy/spectroscopy (STM/STS).^{6,7} Those observations are very interesting because no one observed Coulomb blockade and staircase phenomena in metal–insulator–metal–semiconductor (MIMS) structures before. Radojkovic *et al.*⁶ reported that field-evaporated Au clusters on hydrogen-passivated silicon surfaces revealed Coulomb staircases at room temperature in their tunneling current–voltage (I – V) measurements.

We have also found that ultrasmall Ag clusters grown on Sb-terminated Si(100) surfaces showed clear Coulomb blockade and staircases at room temperature in the region where Ag clusters were densely populated.⁷ However, we could not observe Coulomb staircases in dilutely distributed regions^{7,8} in contrast to the case of Radojkovic *et al.*, and found that the tunneling I – V characteristics showing Coulomb staircases could be well fitted by the metallic double tunnel junction model.⁷ In order to investigate why single electron tunneling (SET) phenomena were seen only in densely populated regions and which electric conduction channels majorly contribute to the Coulomb blockade and staircases in our structures, we selectively manipulated Ag clusters by using a field-induced manipulation method⁹ and measured the local tunneling I – V characteristics of artificially fabricated Ag cluster structures. From the measurement of various structures, we found that lateral tunneling between adjacent clusters is very important and dominantly contributes to the occurrence of the SET phenomena. Furthermore, we fabricated a double tunnel-junction structure showing clear Coulomb blockade and staircases at room temperature through the lateral electric conduction. This discovery is important with a point of view such that we can

fabricate any kinds of surface structures composed of metal clusters to realize various kinds of single electron devices operating at room temperature.

Clean p -type Si(100) with a resistivity of $1 \Omega \text{ cm}$ was obtained via repeated flashing at 1200°C . After preparation of an Sb-terminated Si(100) surface, Ag was deposited on the surface at room temperature for the formation of densely populated Ag nanoclusters. The details of the sample preparation method are described elsewhere.⁸ The STM measurements were performed under the pressure of $\sim 1 \times 10^{-10}$ Torr employing electrochemically etched W tips. In the constant current imaging at 0.5 nA , the sample bias voltage was set to be 2.5 V . At a nominal coverage of 2.0 \AA , which was estimated by a crystal thickness monitor, the sizes of Ag clusters were 3 – 6 nm in diameter and 0.5 – 1.4 nm in height. The average spacing between islands was estimated to be $\sim 3 \text{ \AA}$ at this coverage.⁸ The lateral size of Ag clusters could be overestimated due to the apparent broadening by the tip convolution effect, and accordingly the spacing between clusters could be underestimated. All STM/STS measurements were performed at room temperature.

Most of the densely populated Ag clusters shown in Fig. 1(a) revealed metallic conduction behavior with nonzero current both at $+0$ and -0 V at room temperature. [See the bold line in Fig. 1(e).] Among Ag clusters, however, there were a few such as cluster “ a ” in Fig. 1(a), showing a reproducible I – V curve of SET at room temperature, as reported earlier.^{7,8} The tunneling I – V curve for cluster a shown in Fig. 1(e) reveals a Coulomb gap and weak staircases, which are more clearly visible in the differential conductance (dI/dV) curve.

In order to identify the conduction channel giving rise to the Coulomb blockade and staircases at cluster a , we removed surrounding Ag clusters as shown in Fig. 1(b). A small Coulomb gap and a weak extra feature, most likely staircases, were still visible in the I – V curve of cluster a , as shown in the curve (a') in Fig. 1(f). On the other hand, for well separated Ag cluster a in Fig. 1(c), which was fabricated by removing the clusters “ c ” and “ d ” [see Fig. 1(b)], the tunneling current was suppressed at low bias region, and the weak staircase feature also vanished, as shown in the curve (a''). In addition, the tunneling current was highly sup-

^{a)}To whom correspondence should be addressed; electronic mail: pkh@idea.etri.re.kr

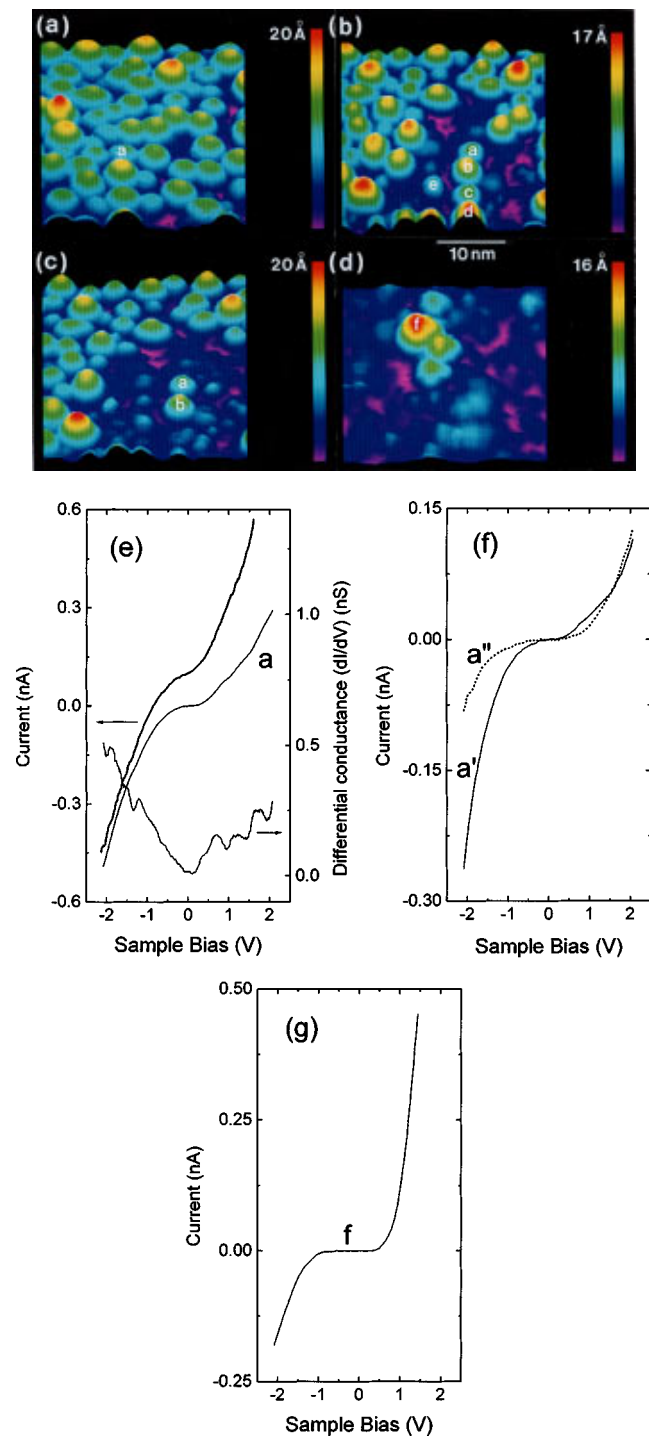


FIG. 1. (a) Densely populated Ag clusters grown on Sb-terminated Si surface at a coverage of 2.0 Å. (b) Linearly chained Ag clusters *a*, *b*, *c*, and *d* fabricated by the field-induced manipulation method. (c) Isolated clusters *a* and *b* after the removal of *c* and *d* clusters in (b). (d) Completely isolated Ag cluster *f* on a bare Sb-terminated Si(100). (e) Typical metallic I - V characteristics (bold line) on Ag clusters at a coverage of 2.0 Å (offset upward for clarity), the Coulomb gap and weak staircase I - V curve (thin line) and conductance (thin line) measured on cluster *a* in (a). (f) Tunneling I - V curves on cluster *a* in (b) (a' , solid line) and (c) (a'' , dotted line). (g) Tunneling I - V curve on cluster *f* in (d).

pressed at negative sample bias in the case of an isolated cluster. The two I - V curves (a' , a'') in Fig. 1(f) were obtained at nearly the same tip positions on Ag cluster *a* such that any position-dependent effect in the I - V measurement⁹ should be excluded. This behavior indicates that the lateral conduction from a particular Ag dot to its adjacent Ag dots,

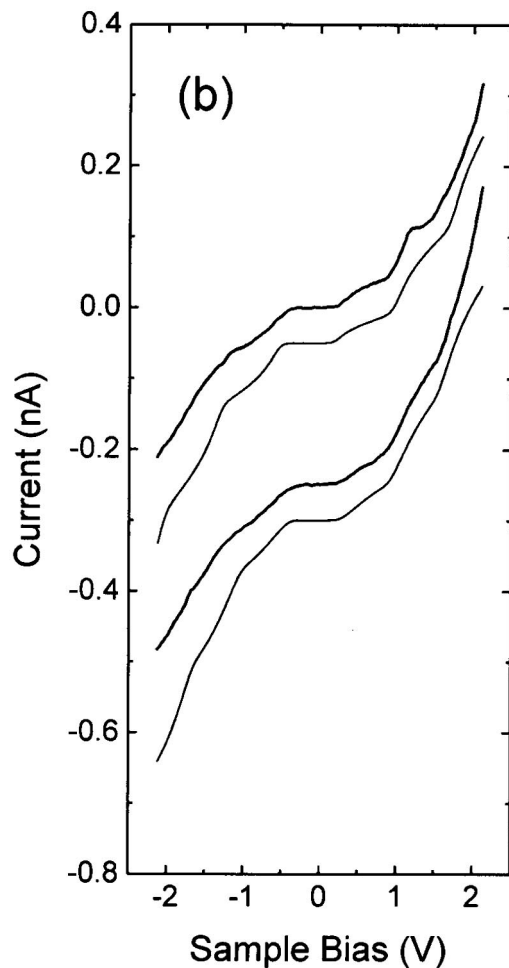
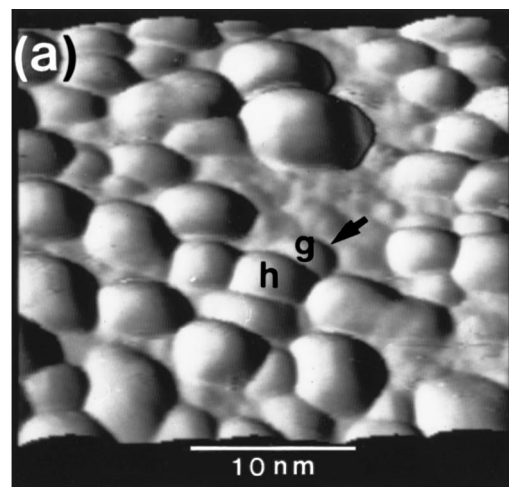


FIG. 2. (a) Perspective view of the STM image of an artificially fabricated double junction single-electron tunneling structure, the ratio between lateral and vertical scale in the image is set to be one. (b) Coulomb staircases (bold lines) with variation of tip heights on cluster *g* in (a), the thin lines denote the least-squares-fitted curves. The fitting parameters of above (below) curve are $C_1=2.13(2.51)\times 10^{-19}$ F, $C_2=4.81(1.04)\times 10^{-20}$ F, $(R_1)_0=8.07(4.06)\times 10^9$ Ω, $(R_2)_0=4.48\times 10^9$ Ω (1.70×10^{10} Ω), $Q_0=-0.22$ (-0.10) e , $\alpha=3.25(5.15)$ (index of nonlinearity, see the Ref. 7), $T=300$ K. The curves are offset for clarity.

for example “ $a\rightarrow b\rightarrow c\rightarrow d$,” plays an important role on the tunneling I - V characteristics of the Ag cluster.

The semiconducting gap of a separated Ag cluster with the field-induced desorption is not clearly resolved as shown in Fig. 1(f) compared to either those in the Ag film of low

coverage (0.4 \AA),⁸ or those in the completely isolated Ag cluster deposited on a bare Sb-terminated Si(100) surface as shown in Fig. 1(d). The tunneling I - V curve in Fig. 1(g) was obtained in the measurement on cluster “f” in Fig. 1(d). The lack of evident semiconducting gap character in the Ag cluster in Fig. 1(c) compared to that in Fig. 1(d) is attributed to the current leakage through the space charge region of silicon to nearby densely distributed metallic cluster regions, as well as due to the tunneling current through residues of Ag clusters such as cluster *e* in Fig. 1(b).

We can thus deduce that the lateral electric conduction from one cluster to the proximate one is very important in the tunneling I - V measurements on Ag clusters. The lateral tunneling through the space charge region seems to be dominant,⁸ because (i) the barrier is much lower than the tunneling barrier through vacuum,¹⁰ and (ii) barrier potentials are smooth and continuous in semiconductors.¹¹ Therefore we can fabricate single electron tunneling structures consisting of Ag nanoclusters via such a lateral tunneling channel at room temperature.

Figure 2 shows clear Coulomb staircases measured on an artificially constructed double tunnel junction structure at room temperature. First, we removed Ag clusters surrounding the cluster “g” indicated by the arrow except cluster “h” which mediates tunneling conduction to dense metallic regions as shown in Fig. 2(a). Next, we performed local I - V measurements on the cluster *g* by varying the tip-to-dot parameters such as the tip-to-dot distance. The two curves (bold lines) in Fig. 2(b) were obtained with variation of tip heights, yielding the change of Coulomb staircases depending on the junction parameters in I - V characteristics. The upper one reveals a much clearer Coulomb staircases compared to the lower one, where the tip-cluster distance is about 1 \AA smaller than that of the lower one. The simplified double junction model can be applied to explain Coulomb staircase phenomena. The compactly distributed Ag clusters including cluster *h* are assigned as the junction electrode 1, which is coupled to dot *g*. The STM tip, which is assigned as the junction electrode 2, is also coupled to cluster *g*. The I - V characteristics on cluster *h* in Fig. 2(a) showed a metallic character without Coulomb blockade or staircases at room temperature, revealing that cluster *h* was directly connected to the silicon substrate via conductively connected dense clusters.

From the least squares fitting of the two I - V curves by using the metallic double-tunnel-junction model,^{12,13} the junction capacitance C_1 is estimated to be 2.13×10^{-19} and 2.51×10^{-19} F for the upper and lower ones, respectively, and another junction capacitance C_2 is estimated to be 4.81×10^{-20} and 1.04×10^{-20} F, respectively. We have assigned the junction 1 and 2 as dot-to-substrate and tip-to-dot junction, respectively, because C_1 was nearly independent of tip height, whereas C_2 and R_2 were found to sensitively depend on it. In order to fit the nonlinear I - V curves, we introduced

the voltage dependent tunneling resistance and nonlinear fitting parameter α due to thermionic emission between Ag clusters or Fowler–Nordheim tunneling.⁷ The fitted C_1 and C_2 values were in good agreement with the geometrically estimated C'_1 ($\sim 2 \times 10^{-19}$ F)¹⁴ and C'_2 ($\sim 3 \times 10^{-20}$ F)¹⁵ values, respectively. The Schottky junction capacitance C_0 by the formation of the metal-semiconductor junction between the central Ag cluster and the silicon substrate was estimated to be much smaller than C'_1 , because the total capacitance of dot-to-substrate should be the sum of C'_1 and C_0 . In our simplified model, the thermionic emission of holes through the Schottky junction of Ag/Si (*p* type) was not included, which should be a dominant conduction path in the case of the isolated cluster.

Field-induced manipulation and the systematic analysis of tunneling I - V characteristics suggested that the lateral tunneling between adjacent clusters should be a major contribution to the conduction which enables the Coulomb staircases in the tunneling I - V measurements. This result can be further utilized for the construction of nanoscale single-electron devices composed of lateral conduction channels, which operate at room temperature especially under the condition of highly suppressed thermionic emission between the cluster and substrate.

The authors wish to thank Professor Y. Kuk (S.N.U.) for his helpful comments and discussion. This work has been supported by the Ministry of Information and Communications, Korea.

¹R. Ludeke, T.-C. Chiang, and T. Miller, *J. Vac. Sci. Technol. B* **1**, 581 (1983).

²R. M. Feenstra and P. Mårtensson, *Phys. Rev. Lett.* **61**, 447 (1988).

³D. L. Carroll, M. Wagner, M. Ruhle, and D. A. Bonnelli, *Phys. Rev. B* **55**, 9792 (1997).

⁴P. N. First, J. A. Stroscio, R. A. Dragoset, D. T. Pierce, and R. J. Celotta, *Phys. Rev. Lett.* **25**, 1416 (1989).

⁵M. Valden, X. Lai, and D. W. Goodman, *Science* **281**, 1647 (1998).

⁶P. Radojkovic, M. Schwartzkopff, M. Enachescu, E. Stefanov, E. Hartmann, and F. Koch, *J. Vac. Sci. Technol. B* **14**, 1229 (1996).

⁷K.-H. Park, J. S. Ha, W. S. Yun, M. Shin, K. Park, and E.-H. Lee, *Appl. Phys. Lett.* **71**, 1469 (1997).

⁸K.-H. Park, J. S. Ha, W. S. Yun, and E.-H. Lee, *Surf. Sci.* **415**, 320 (1998).

⁹K.-H. Park, J. S. Ha, W. S. Yun, and E.-H. Lee, *J. Vac. Sci. Technol. A* (in press).

¹⁰H. H. Weitering, J. P. Sullivan, R. J. Carolissen, R. Perez-Sandoz, W. R. Graham, and R. T. Tung, *J. Appl. Phys.* **79**, 7820 (1996).

¹¹S. M. Sze, *Physics of Semiconductor Devices* (Wiley, New York, 1981).

¹²D. V. Averin and K. K. Likharev, *Mesoscopic Phenomena in Solids*, edited by B. L. Altshuler, P. A. Lee, and R. A. Webb (North-Holland, New York, 1991), Chap. 6.

¹³M. Amman, R. Wilkins, E. Ben-Jacob, P. D. Maker, and R. C. Jaklevic, *Phys. Rev. B* **43**, 1146 (1991).

¹⁴By using the parallel plate approximation ($C = \epsilon_0 \epsilon_r A/d$), taking $\epsilon_r = 11.9$ (silicon), $A = (\pi/2) \times 6 \text{ \AA} \times 11 \text{ \AA}$, $d = 5 \text{ \AA}$ from the size of the smaller cluster *g* and the spacing distance, where we assumed that the silicon was inserted between Ag clusters *g* and *h* as a crude approximation, since $\epsilon_r(\text{Si}) \gg \epsilon_r(\text{vacuum})$.

¹⁵Taking $\epsilon_r = 1$ (vacuum), $A = \pi \times 11 \text{ \AA} \times 11 \text{ \AA}$, and assuming $d = 10 \text{ \AA}$.